



Published in final edited form as:

Lab Invest. 2020 April ; 100(4): 630–642. doi:10.1038/s41374-019-0338-2.

## Shp2-mediated MAPK pathway regulates Np63 in epithelium to warrant corneal innervation and homeostasis

Yuka Okada<sup>1,2</sup>, Yujin Zhang<sup>1</sup>, Lingling Zhang<sup>1</sup>, Lung-Kun Yeh<sup>3</sup>, Yen-Chiao Wang<sup>1</sup>, Shizuya Saika<sup>2</sup>, Chia-Yang Liu<sup>1</sup>

<sup>1</sup>Indiana University School of Optometry, Bloomington, Indiana USA

<sup>2</sup>Department of Ophthalmology, Wakayama Medical University, School of Medicine, Wakayama, Japan

<sup>3</sup>Department of Ophthalmology, Chang-Gung Memorial Hospital, Linko, Taiwan

### Abstract

Corneal nerve fibers serving sensory, reflex and neurotrophic functions sustains the corneal homeostasis and transparency to warrant the normal visual function. It remains unknown whether corneal epithelium is also reciprocally important for the corneal innervation. Herein, we generated a compound transgenic mouse strain, *K14rtTA;tetO-Cre (TC);Shp2<sup>flox/flox</sup>*, in which *Shp2* was conditionally knocked out from the K14-positive cells including corneal epithelium (*Shp2<sup>K14ce-cko</sup>*) upon doxycycline (dox) administration. Our data revealed that *Shp2<sup>K14ce-cko</sup>* resulted in corneal denervation. More specifically, the corneal epithelium thickness and corneal sensitivity reduced dramatically in *Shp2<sup>K14ce-cko</sup>* mice. In addition, corneal epithelial debridement wound healing was delayed substantially in the mutant mice. These defects manifested in *Shp2<sup>K14ce-cko</sup>* mice resemble the symptoms of human neurotrophic keratopathy. Our *In vitro* study unveiled that neurite outgrowth of the mouse primary trigeminal ganglion cells (TGCs) was inhibited as co-cultured with mouse corneal epithelial cells (TKE2) transfected by *Shp2*-, *Mek1/2*-, or *Np63*-targeted siRNA but not by *Akt1/2*-targeted siRNA. Furthermore, *Np63* RNA interference down-regulated *Ngf* expression in TKE2 cells. More interesting, co-transfection experiments revealed that Shp2 tightly monitored Np63 protein level in HEK293 and TKE2 cells. Taken together, our data suggested that Shp2-mediated MAPK pathway regulated Np63, which in turn positively regulated *Ngf* in epithelium to warrant corneal innervation and epithelial homeostasis

### Keywords

Shp2; MAPK; Np63; corneal epithelium; corneal innervation

Users may view, print, copy, and download text and data-mine the content in such documents, for the purposes of academic research, subject always to the full Conditions of use:[http://www.nature.com/authors/editorial\\_policies/license.html#terms](http://www.nature.com/authors/editorial_policies/license.html#terms)

Correspondence should be addressed to Yuka Okada, yokada@wakayama-med.ac.jp and Chia-Yang Liu; liuchia@iu.edu.

## Introduction

The vertebrate cornea is a dome-shaped transparent outer surface of the eye. It contains five anatomic layers, which are the epithelium, Bowman's layer, the stroma, Descemet's membrane and the endothelium. As the outermost layer, corneal epithelium (CE) consists of non-keratinized, stratified squamous epithelial cells, which are held together by tight junctions, to form an effective barrier against fluid loss and pathogen penetration [1]. Additionally, the CE is one of the most sensitive structures in the body as it is densely innervated with corneal nerve fibers [2]. The majority of the corneal nerves are afferent sensory nociceptors, derived from the first (ophthalmic) division of the fifth cranial (CNV1 or trigeminal) nerve [3]. These nerve fibers project into peripheral corneal stroma from the corneoscleral limbus. After entering the cornea, the main stromal nerve bundle gives rise through branching to smaller stromal nerves to form a mid-stromal plexus and then sub-epithelial plexus, which supplies all layers of the CE [2,4,5]. The proper patterning of corneal innervation renders the cornea to respond quickly to irritation, touch and pain, thus protecting the cornea from the potential harmful external environment and injuries. Moreover, corneal nerves are involved in modulating blink reflexes and tear fluid production that maintain corneal proper hydration [6,7]. Therefore, corneal innervation is crucial for sustaining corneal homeostasis and biological functions [8,9].

It has been postulated that constantly direct interaction between the CE cells and corneal nerves exists during corneal development and homeostasis [10,11]. Several lines of *in vitro* evidence from co-culture of trigeminal ganglion cells (TGCs) and CE cells indicated that these two cell types do support one another through the secretion of trophic factors [12–17]. Substance P (SP) is one of important trophic factors and may associate with other growth factors, such as epidermal growth factor (EGF), to promote migration and proliferation of corneal epithelial cells during corneal healing [13]. Likewise, interaction between corneal nerves and the CE cells itself is thought to be necessary for proper nociception and corneal protection [3]. It is known that neurotrophin-3 (NT3) derived from cornea can promote the expression of transient receptor potential A1 (TRPA1) ion channels in the corneal nerves, which enhances CNV1 innervation during embryonic corneal development [18]. Moreover, it has been proposed that CE cells function as surrogate Schwann cells for their sensory nerves during homeostasis and in response to injury" [11]. Therefore, the close interaction and interdependent relationship properly maintained between the CE cells and corneal nerves are required to grant a healthy and functional cornea. Any disruption of this relationship or interaction would have deleterious effects on the anatomic integrity of the cornea, which may lead to persistent corneal disorders such as neurotrophic keratopathy (NK).

NK is a rare degenerative disease with reduction or absence of corneal sensation characterized by progressive damage to CE cells that can result in corneal perforation, with consequent loss of vision [19]. NK can be caused by a wide range of ocular and systemic diseases including congenital corneal anesthesia, dry eyes, and decreased eye blinking due to impaired corneal sensitivity, trauma, surgery, herpetic virus infection, misuse of topical medications, use of contact lenses and even systemic conditions such as diabetes or vitamin A deficiency [20–22]. Currently, the diagnosis and treatment of NK are the most complex

and challenging aspects of this disease, as the cellular and molecular pathogenesis of the NK syndrome remains elusive and a satisfactory therapeutic approach is not yet available [23]. Therefore, understanding the role of key signaling molecules during signaling transductions which modulating the interplay between CE cells and trigeminal nerves will facilitate the development of novel treatments for this disease. Among these signaling molecules, Shp2 has been complicated in multiple signaling transductions that may participate in CE stratification and corneal nerve innervation [24].

Shp2 is a member of Src-homology 2 domain-containing protein tyrosine phosphatase family [25]. It is widely expressed in most tissues and plays a fundamental role in various cell signal transductions that control multiple important cellular events, such as proliferation, apoptosis and migration [26–29]. As a major mediator of cellular signaling transductions, Shp2 is in a naturally auto-inhibited condition and is activated once an extracellular ligand like EGF binds EGF receptor (EGFR). When Shp2 binds the phosphor-EGFR (active form), the scaffolding proteins, Grb2 and Gab1, are able to form a functional complex relaying signals to downstream components, leading to the initiation or/and regulation of the cellular processes like cell proliferation [30]. We previously reported that genetic ablation of *Shp2* in K14-positive epithelial cells disrupted corneal epithelial stratification during mouse development [24]. In current study, we further investigate the role of Shp2 during corneal epithelial homeostasis and corneal nerve innervation. Our data show that *Shp2* ablation in K14-positive epithelial cells impaired corneal epithelial maintenance; delayed epithelial debridement wound healing and caused CE nerve denervation with loss/decrease of corneal sensation, resembling the symptoms of NK. We also establish the concept that Shp2 signals through MEK/ERK pathway in the epithelium is critical for the maintenance of corneal epithelial innervation and homeostasis.

## Materials and methods

### Mice.

Compound transgenic mouse strains *K14rtTA;tetO-Cre;Shp2<sup>flox/flox</sup>* and *K14rtTA;tetO-Cre;Shp2<sup>flox/flox</sup>;Thy1-YFP* were generated through the natural mating of single transgenic mouse lines *K14-rtTA* [31], *tetO-Cre* [32], *Thy1-YFP* [33] and *Shp2<sup>flox/flox</sup>* [34], respectively. *Shp2* ablation in the K14-positive cells was achieved by administering doxycycline (Dox) chow to *K14rtTA;tetO-Cre;Shp2<sup>flox/flox</sup>* transgenic mice in the dam for 14 days from postnatal day (P60) to P74. Mouse corneas (N=6) were collected after dox-induction 4, 6, 10, 14 day, respectively. Genetic knockout of *Shp2* was also performed in compound transgenic mice *K14rtTA;tetO-Cre;Shp2<sup>flox/flox</sup>;Thy1-YFP* by Dox treatment from P23 to P33 and corneas (N=6) were collected at P33. YFP-positive corneal nerve fiber images were taken by Zeiss Axio Zoom V16 stereomicroscope. All experiments involving mice were approved by the Animal Care and Use Committee of Indiana University and conducted in accordance with the Association for Research in Vision and Ophthalmology Statement for the Use of Animals in Ophthalmic and Vision Research.

### Hematoxylin and Eosin (H&E) Histological staining analysis

Enucleated mouse eyes were fixed overnight in 4% paraformaldehyde (PFA) diluted in 1X phosphate buffered saline (PBS), followed by dehydration in a series of ascending alcohol (50%, 75%, 95% and 100%) and paraffin embedding. Deparaffinized sections (5µm) were stained with H&E reagent following protocol as previously described [24].

### Functional assay of corneal sensitivity in mice

Corneal sensitivity of alive experimental mice was measured by the handheld esthesiometer (Cochet-Bonnet) (Luneau Ophthalmogica, France). Mouse eyes (N=6) of Dox-treated *K14-rtTA;TC;Shp2<sup>WT/WT</sup>* (control) and *K14-rtTA;TC;Shp2<sup>flox/flox</sup>* (*Shp2<sup>K14ce-cko</sup>*), respectively, were measured 3 times and the length of nylon filament that elicited eyelid blinking was recorded and converted into average threshold pressure (g/mm<sup>2</sup>) according to the formula provided by manufacturer. The normal corneal sensitivity ranges from 0.4 to 0.7g/mm<sup>2</sup> (or 60–45 mm nylon filament length) [35].

### Corneal whole mount immunostaining

The mouse corneas were fixed overnight in 4% paraformaldehyde diluted in 0.1M phosphate-buffer. The fixed corneas were carefully cut into a clover leaf shape and incubated in 0.2% sodium borohydride in 1x PBS for 1hr at room temperature. After three washes with 1x PBS, the corneas were incubated in 2N HCl, 0.5% TritonX-100® in 1x PBS for 1hr at room temperature. After one wash with 0.1M phosphate buffer (pH 7.4) and two washes with 1x PBS, the corneas were incubated in 1µg/ml bovine serum albumin in 50% TD (0.5% DMSO, 0.5% TritonX-100®, and 2.5% Dextran 40 in PBS) for 15 min at room temperature. The corneal samples were probed with neuron-specific βIII-tubulin (Tuj1) northernlight™ NL-557-conjugate antibody at 1:10 dilution (R&D Systems; Cat#: NL1195R) for 24hrs at 4°C. After twice washes with 50%TD and one wash with 1x PBS. The corneal samples were mounted and observed under EVOS FL Auto Cell Imaging System (Invitrogen-Thermo Fisher Scientific).

### Transmission Electron Microscopy

Corneal samples were fixed in 0.1M cacodylate buffer (pH7.4) containing 3% glutaraldehyde and 2% paraformaldehyde for 2hrs at 4°C and then were preserved in 0.1M cacodylate buffer (pH 7.4) containing 0.5% glutaraldehyde at 4°C overnight. After re-fixation in 1% osmium tetroxide (OsO<sub>4</sub>) for 1hr at 4°C, corneal samples were washed in 0.1M cacodylate buffer (pH 7.4) three times for 10 min each, and then dehydrated in a graded ethanol series and embedded in Epon 812 epoxy resin (Polysciences, Inc., Warrington, PA). Ultrathin 50-nm sections were stained with uranyl acetate and lead citrate and images were photographed with a Hitachi 7500 Transmission Electron Microscope (Hitachi, Tokyo, Japan) equipped with AMT Digital camera.

### Co-culture of primary trigeminal ganglia and siRNA transfected TKE2 cells

TKE2 cells (ECACC 11033107) were cultured in six-well plates with 2ml Keratinocyte-serum free medium (KSFM, Gibco #17005–042). At 30–40% cell confluence, TKE2 cells were transfected with different siRNA (10nM) using lipofectamine RNAiMAX (Invitrogen,

Cat: #13778) following the manufacturing protocol to knock down gene expression of *Shp2*, *Mek1/2*, *Akt1/2* and *Np63*, respectively. TKE2 cells transfected with non-target control siRNA were used as negative control. The siRNAs used in this study were listed in supplementary Table 1.

Primary culture of trigeminal ganglion cells was prepared according to a method previously described [36] with a minor modification: trigeminal ganglia from five C57BL/6 mice at P10 were dissected, washed with ice-cold DMEM/F12, and enzymatically digested with 0.1% collagenase (Type I, Sigma, #C0130)/DMEM/F12 for 30min at 37°C followed by treatment with 0.05% trypsin/EDTA-HBS (Invitrogen, #25300-054) for 40min at 37°C. The digested ganglia were washed once with DMEM/F12 supplemented with 10% fetal calf serum and triturated with fire polished glass pipettes. The cell suspension was centrifuged at 2,000 rpm for 2min. Cell pellets were re-suspended and seeded in DMEM/F12 supplemented with 10% fetal calf serum in 6-well plates ( $\sim 2.0 \times 10^5$  cells/well). The next day, cells were treated with 3 $\mu$ g/ml of mitomycin-C at 37°C for 2hrs, washed with PBS. Then siRNA treated-TKE2 cells were added ( $\sim 4.0 \times 10^4$  cells/well) and co-cultured in KSFM for another 3 days.

### Measurement of neurites outgrowth

Under stereomicroscope, each co-culture well of trigeminal ganglion cells with different siRNA transfected TKE2 cells was randomly selected for taking photographs. The length of neurites from each co-culture (n=90) was measured by a COMCURVE-9Jr pen-type curvimeter (Koizumi Sokki Mfg. Co., Ltd). Data from 3–5 times repeated experiments were analyzed by the Student's *t*-test.

### Transfection of *Shp2* and *Np63* plasmid DNAs in HEK293, HTCE, or TKE2 cells

HEK293 cells (ATCC® CRL-1573™) cultured in six-well plates with DMEM medium containing 10% fetal bovine serum were co-transfected with a various amounts of *CMV-Shp2WT* (Addgene, #8381) and *Np63-Flag* (Addgene, #26979) at 70% confluence as indicated in Fig.5A using calcium phosphate transfection kit (Thermal-Fisher Cat: K278001) according to the manufacturing protocol. 48hrs post-transfection, total protein isolated from cell lysates was subjected to western blotting to detect the expression of *Shp2* and *Np63*. To test whether *Shp2* regulates *Np63* protein stability, HEK293 cells seeded in six-well plates were co-transfected with 1 $\mu$ g/well *CMV-Shp2WT* and 2 $\mu$ g/well *Np63-Flag* and treated with a different amount of MG132 (Sigma-Aldrich, Cat:1211877-36-9) as indicated in Fig.5B. 48hrs after transfection, protein level of *Shp2* and *Np63* was examined by western blotting analysis.

### Immunocytofluorescence staining

TKE2 cells, cultured in four-well chamber slides with KSFM medium were transfected with 0.5 $\mu$ g *Shp2-EGFP* plasmid (Addgene, #12283) using lipofectmine 2000 reagent (Invitrogen, Cat:11668-030) via reverse-transfection procedure according to the manufacturing protocol. 48hrs post-transfection, TKE2 cells were transiently fixed in 4% paraformaldehyde, blocked with 3% bovine serum albumin in PBS containing 0.05% NP-40 for 1h at room temperature, and then incubated overnight at 4°C with primary antibodies diluted in the same buffer. After three washes in 1x PBS containing 0.1% Tween 20 (PBST), slides

were incubated at room temperature for 1h with Alexa Fluor 488- and/or Alexa Fluor 555-conjugated secondary antibodies (Life Technologies) and 1µg/ml DAPI as a nuclear counterstain. Following incubation, the slides were washed with PBST and mounted with Mowiol (Sanofi-Aventis). Sections were examined and photographed using a Zeiss Axio Observer Z1 microscope equipped with an Axiocam Mrm camera or EVOS FL Auto Cell Imaging System (Invitrogen-Thermo Fisher Scientific). Primary antibodies, mouse monoclonal anti-Flag antibody (sigma, Cat: F3040) and rabbit anti- Np63 (Abcam, Cat: Ab166857) were used to detect Shp2 and Np63 expression, respectively. The secondary antibodies, goat anti-mouse IgG-Alex488 (Thermo-Fisher Scientific, A-11001), goat anti-rabbit IgG-Alex555 (Thermo-Fisher Scientific, A27039) were used to assist in the detection by the immunostaining.

### Healing of an epithelial defect in *in vivo* mouse cornea

Under general anesthesia, a round epithelial defect (2.0 mm in diameter) was produced in the central cornea of the right eye of a mouse as using a skin biopsy trephine and microsurgical blade in each experiment as previously reported [37,38]. At specific intervals during the healing process, each cornea was processed for evaluation of the epithelial defect closure. Epithelial closure the cornea was evaluated by measuring the size of green fluorescein-stain of the defect of the epithelium as previously reported [39].

### Real-time quantitative PCR (RT-qPCR) and reverse transcription PCR (RT-PCR)

Total RNA (10µg) was isolated from TKE2 or HEK293 cells using Trizol reagent (Invitrogen), then annealed to random primers and reverse transcribed with avian reverse transcriptase (RT) kits (Promega), according to the manufacturer's instructions. RT-PCR was performed using C1000 Touch Thermal cycler (Bio-Rad Laboratories Inc.). 30–35 PCR cyclers were carried out to detect the expression of Bmp4 and housekeeping gene *Gapdh*. RT-qPCR was performed using the CFX96 real-time system equipped with a C1000™ Thermal Cycler (Bio-Rad Laboratories Inc.). After the initial 3mins denaturing step at 95°C, 40 subsequent cycles at 95°C lasting 15s, 62°C for 15s, and 72°C for 20s were performed. The cycle threshold values were used to calculate the normalized expression of genes of interest against *Gapdh* using Q-Gene software. RT-qPCR primer *Shp2*-F 5' GTCCACCACAAGCAGGAGAG and *Shp2*-R GAACGTCGATGTCACAGTCC was used for *Shp2* expression in TKE2 cells. Primer *Np63*-F 5' GGAAAACAATGCCCAGACTCAA and *Np63*-R 5' GGTCAGTGGTCTGAGTCT was used to examine *Np63* expression in TKE2 cells. Primer m*Ngf*-F 5' CTGTGCCTCAAGCCAGTGAA and m*Ngf*-R 5' TCACTGCGGCCAGTATAGAA was used to examine *Ngf* expression in TKE2 cells. Primer *Gapdh*-F 5' AGGTGGTGAAGCAGGCATCT and *Gapdh*-R 5' TTA CTCTTGGAGGCCATGT was used to detect *Gapdh* expression in TKE2 cells.

### Western blotting analysis

TKE2 or HEK293 cells were homogenized in RIPA buffer (50mM Tris base, 150mM NaCl, 0.5% deoxycholic acid-sodium salt, 2% SDS, and 1% NP40, pH 7.5) containing 1x protease inhibitor cocktail (Sigma P8340). Cell lysates (20µg) from each sample were separated on a 4–20% linear gradient Tris-HCl denaturing polyacrylamide Ready Gel (Bio-Rad) and

transferred to PVDF membrane (Whatman). Membranes were blocked with 5% nonfat milk in TBST (10mM Tris-HCl pH 8.0, 150mM NaCl, 0.05% Tween 20) and probed with primary antibody in the same buffer overnight at 4°C. After three washes in TBST, membranes were probed with HRP-conjugated secondary antibody for an hour at room temperature and bond second antibody was further detected using an enhanced chemiluminescence assay (Supersignal West Pico, #34080; Thermo-Fisher Scientific) and examined and photographed using a VersaDoc 4000MP imaging system (Bio-Rad). Primary antibodies, rabbit anti-Shp2 (D50F2) (cell signaling, Cat: 3397P), rabbit anti-Np63 (Abcam, ab166857), rabbit anti-Ngf (LSBio LS-C171793), and goat anti- $\beta$ -actin (Santa Cruz, sc-1616) were used to examine expression of Shp2, Np63, Ngf, and  $\beta$ -actin, respectively. The secondary antibodies, goat anti-rabbit IgG-HRP (Thermo-Fisher Scientific, G-21234), donkey anti-goat IgG-HRP (Thermo-Fisher Scientific, A16005) were used to assist in the detection by western blots.

### Statistical analysis

A two-tailed Student's *t*-test (Excel, Microsoft, Redmond, WA, USA) was used to analyze the significance of difference;  $P < 0.05^*$  was considered statistically significant and  $P < 0.01^{**}$  was considered highly statistically significant.

## RESULTS

### Corneal epithelial thinning and reduction of nociception in *Shp2*<sup>K14ce-cko</sup> adult mice

To explore the role of Shp2 in corneal epithelial homeostasis, Dox chow was administered in the dam to *K14-rtTA;TC;Shp2*<sup>WT/WT</sup> (control) and *K14-rtTA;TC;Shp2*<sup>flox/flox</sup> (*Shp2*<sup>K14ce-cko</sup>) adult mice (Fig. 1A) from postnatal day 60 (P60) for different time points as mentioned in material and method. Histologic analysis by H&E stain clearly showed that the CE cells maintained 6–7 cell layers in control mice (Fig. 1B, 1D, 1F, 1H). In contrast, except for those with 4 days Dox treatment (Fig. 1C), the CE cells were dramatically reduced to 2–3 layers in *Shp2*<sup>K14ce-cko</sup> mice after Dox treatment (Fig. 1E, 1G, 1I). These suggested that CE homeostasis was disrupted in *Shp2*<sup>K14ce-cko</sup> mice. In addition, deletion of *Shp2* in basal CE cells of *Shp2*<sup>K14ce-cko</sup> mice caused a progressive loss of corneal sensation starting from 10 days of Dox administration as examined by Cochet-Bonnet aesthesiometer (Fig. 1J). We found that the anatomical changes of CE in *Shp2*<sup>K14ce-cko</sup> mice were noticed at day 6 and then the reduction of corneal sensation occurred on day 10 after Dox treatment (Fig. 1E, 1J). This result demonstrated that disruption of CE in *Shp2*<sup>K14ce-cko</sup> mice significantly affected normal corneal sensation and corneal homeostasis.

### Shp2 deficiency results in corneal denervation in *Shp2*<sup>K14ce-cko</sup> adult mice

The reduction of corneal sensation after *Shp2* ablation implied that corneal innervation might be impaired in *Shp2*<sup>K14ce-cko</sup> mice. To address this concern, corneal innervation was examined by whole-mount corneal immunofluorescent staining of Tuj1, a marker for sensory nerve fibers. Our data clearly showed that the density of corneal nerve fibers was dramatically reduced in *Shp2*<sup>K14ce-cko</sup> as compared to littermate controls with 10 days' dox administration (Compare Fig. 2D, 2F with 2C, 2E). This result suggested that Shp2 in basal

corneal epithelial cells of adult mice played critical role in the maintenance of corneal innervation.

Next, we took a closer look regarding the ultrastructure of corneal innervation by the transmission electron microscopy (TEM) in adult mice (Fig 3). Control corneal epithelium exhibited healthy nerve bundles in the epithelial basal layer (Fig. 3A, A') and nerve fibers in subbasal layers (Fig. 3C, C'). On the contrary, *Shp2*<sup>K14ce-cko</sup> mutant mice displayed degeneration in both nerve bundles and fibers (Fig. 3B, B', D, D').

In another set of experiments, we generated the quadruple transgenic mouse strain, *K14rtTA;TC;Shp2*<sup>flox/flox</sup>; *Thy1-YFP*, in which yellow fluorescent protein (YFP) driven by Thy1 promoter is strongly expressed in motor and sensory neurons. We administered this strain and *Thy1-YFP* control mice with Dox chow from P23 to P33 to examine the possible damage in corneal innervation after *Shp2* ablation. YFP fluorescent images clearly demonstrated that Thy-1-positive corneal nerve networks were detected in control corneas as judged by nerve fibers/branches and nerve ending properly organized in the suprabasal layers, basal layer, epithelial-stromal junctions, anterior and posterior stromal layers. In contrast, the Thy-1-YFP signal either was fragmented or absent in *Shp2*<sup>K14ce-cko</sup> mice (Figs. 4. & 5). Compared with what we observed in adult mice, these data suggest that more severe damage in corneal innervation after *Shp2* ablation occurred in young mice than those in elder ones. Taken together, these observations pointed out that *Shp2* deficiency in basal corneal epithelial cells resulted in corneal denervation. This is consistent with loss/decrease of corneal sensation in the *Shp2*<sup>K14ce-cko</sup> mice.

#### **Knockdown of MEK1/2 expression decreases neurite outgrowth of trigeminal ganglia *in vitro***

It is known that Shp2 transmits signals mainly through Mek and/or Akt in various cell types [40]. To define Shp2 downstream signaling pathway in CE cells for corneal innervation, we measured neurite outgrowth of mouse primary trigeminal ganglia co-cultured with different siRNA transfected-TKE2 cells, in which *Shp2*, *Mek1/2* or *Akt1/2* was knocked-down with specific siRNA transfection, respectively. As shown in Fig.6, TKE2 transfected with either *Shp2* siRNA or *Mek1/2* siRNA remarkably decreased the length of neurite of the primary cultured trigeminal ganglia as compared with control siRNA transfected-TKE2. However, TKE2 transfected with *Akt1/2* siRNA had no significance on the length of neurite from TGCs. These data suggested that Shp2 might transmit through MEK/ERK, but not PI3K/AKT downstream signaling to affect the behavior of corneal epithelial cells and corneal innervation.

#### **Knockdown of *Np63* affected *Ngf* expression in TKE2 cells and neuron outgrowth of trigeminal ganglia *in vitro***

To explore the downstream target of Shp2-MEK-ERK signaling transduction in corneal epithelium, which may associate with corneal innervation, the transcription factor, *Np63* was selected to test this possibility since we previously found that *Np63* expression was dramatically reduced in *Shp2*<sup>K14ce-cko</sup> mice [24]. Indeed, qRT-PCR showed that *Np63* mRNA level was downregulated to ~40% in *Shp2* siRNA-treated TKE2 cells (Fig.7A).



Western blot analysis confirmed Np63 protein level was also decreased in *Shp2* siRNA treated-TKE2 cells (Fig.7B). In addition, co-culture experiments revealed that as compared with the control siRNA (Fig.7C), either *Shp2* siRNA (Fig.7D) or *Np63* siRNA transfected-TKE2 cells (Fig.7E) significantly reduced the length of neurite outgrowth of primary TGCs (Fig.7F).

This data implicated that part of the interaction between TKE2 cells and TGCs through Shp2 might be through diffusible factors. Interestingly, indeed, Ngf protein expression level was down-regulated in Np63 siRNA (20 & 50 nM) transfected TKE2 cells (Fig.8A, lanes 3&4). Likewise, *Ngf* mRNA level was also reduced ~90% in *Shp2*<sup>K14ce-cko</sup> mice as compared to that in *Shp2*<sup>WT</sup> littermate (Fig 8B). Taken together, our data suggested that Shp2→MEK→ Np63 signaling axis at least in part positively regulated Ngf in corneal epithelium which was important for the maintenance of corneal epithelial innervation.

### Shp2 tightly monitors Np63 expression in cultured cells

To understand the mechanism by which Shp2→MEK signaling regulated Np63 expression in corneal epithelium, HEK293 cells were co-transfected with CMV-*Shp2* cDNA and CMV-*Np63* cDNA plasmids at different ratio for 48 hrs. Western blot analysis revealed that Shp2 controlled Np63 protein levels in a dosage dependent manner (Fig. 9). As shown in lane 2 and lane 3 of Fig.8A, co-transfection of HEK293 cells with Np63 plasmid DNA (2μg) and *Shp2* plasmid DNA (ranging from 0.01–0.1μg), Np63 protein expression levels were upregulated. However, *Shp2* plasmid concentration greater than 1μg caused downregulation of Np63 protein (Fig.9A, lanes 4–6). However, MG132, a proteasome inhibitor, attenuated the inhibitory effect of high dosage Shp2 to Np63 protein (Fig.9B). More interestingly, co-transfection of the human corneal epithelial cell line (HTCE) with CMV-*Shp2* cDNA and CMV-*Np63* cDNA plasmids indicated that Shp2 protein (red) and Np63 protein (green) were exclusively presented in HTCE cells as shown by immunocytofluorescent staining (Fig. 9C). These data suggested that at normal/physiological condition, Np63 protein level was positively regulated by Shp2. However, overexpression of Shp2 caused degradation of Np63 protein. Taken together, our data suggested that Np63 was tightly regulated by Shp2 in mouse corneal epithelial cells.

### Shp2 deficiency delays corneal debridement wound healing in *Shp2*<sup>K14ce-cko</sup> adult mice

Our data demonstrated that Shp2 ablation impaired corneal epithelial homeostasis and sensation in *Shp2*<sup>K14ce-cko</sup> adult mice. These defects might affect corneal debridement wound healing. To test this hypothesis, we performed a 2.0 mm diameter corneal epithelial debridement and the re-epithelialization was evaluated every 6 hours. We found that wound healing process in *Shp2*<sup>K14ce-cko</sup> adult mice was significantly hindered as compared with control mice. Fig.9A showed that wound area was healed at 36–42 hours post wound in control mice, while the mutant corneas still have uncovered defects even at 48 hours after wound (Fig.10A, B). H&E staining showed that 4–5 epithelial cell layers formed in the control mice at 48 hours post wound, while there were no corneal epithelial cells covered in the *Shp2*<sup>K14ce-cko</sup> mice (Fig. 10C). These data was consistent with the notion that indeed cornea denervation and thinner epithelium delayed wound healing in *Shp2*<sup>K14ce-cko</sup> mouse.

## Discussion

In current study, we, for the first time, demonstrated that *Shp2* ablation in corneal basal epithelial cells of adult mice resulted in thinner epithelium, nerve denervation, reduction of nerve sensation and retardation of corneal debridement wound healing in the *Shp2<sup>K14ce-cko</sup>* mice. These defects resemble the clinical characteristics of neurotrophic keratopathy (NK) in human. Furthermore, co-culture experiments indicated that either knockdown of *Shp2*, *Mek1/2* or *Np63* in corneal epithelial cells encumbered neurite outgrowth of mouse primary trigeminal ganglia *in vitro*. At the molecular level, we found that *Shp2* tightly regulated the *Np63* protein level probably through MEK-ERK signaling pathway in corneal epithelial cells. Therefore, *Shp2* expression in corneal basal epithelial cells is of paramount importance in maintaining corneal homeostasis and innervation.

To study the pathophysiologic mechanism and the interaction between corneal epithelium and trigeminal nerves *in vivo* of NK, some experimental animal models were produced by trigeminal denervation and investigated the consequence of cornea [41,42]. Recently, we developed a new NK mouse model by coagulating the first branch of the trigeminal nerve [36]. Therefore, most of these works were focused on the effect of impaired trigeminal nerves to the development and homeostasis of corneal epithelium. On the other hand, it is believed that close relationships exist between corneal epithelial cells and nerve fibers during corneal development and homeostasis [23,43,44]. For instance, corneal epithelial cells and sensory nerves work together to form specialized synapse-like structures in corneas [7]. Corneal epithelial cells function as surrogate Schwann cells for their sensory nerves [11]. However, not much attention has been paid to how corneal epithelial cells affect nerve innervation. There was no available animal model generated by specifically attacking the corneal cells and exploring the response of corneal nerves. The mouse strain, *K14rtTA;TC;Shp2<sup>flox/flox</sup>* used in current study might be the first transgenic animal model to fill this gap. In this model, *Shp2* gene is conditionally knocked out specifically in basal epithelial cells (K14 expressing cells) by Dox induction. Consequently, the homeostasis of corneal epithelium was disrupted after *Shp2* deletion, leading to thinner epithelium in the adult mutant mice (Fig. 1B–H). Notably, the phenotype of corneal epithelial thinning was followed by corneal denervation and reduction of corneal sensation (compare Fig. 1B–H with 1J). These data implied that sustaining the intact corneal epithelial stratification and integrity were crucial for preservation of corneal innervation and sensation. So this mouse strain could serve as a useful tool to study several critical questions such as what and how signals, signaling molecules or neurotropic factors derived from corneal epithelial cells triggering and/or involving in the pathogenesis of NK syndrome.

Taking advantage of our triple transgenic mouse strain, *K14rtTA;TC;Shp2<sup>flox/flox</sup>* and co-culture *in vitro* experiments, we concluded that the signals from activated tyrosine protein kinase receptor (for example, phosphor-EGFR) mediated by *Shp2*-MEK-ERK- *Np63* signaling axis in corneal K14-expressing cells were critical both for the corneal epithelium maintenance and innervation in adult mice. It has been well documented that *Np63* expressed in basal epithelial cells played essential roles in epithelial stratification and homeostasis in corneas and skins via multiple mechanisms such as promoting cell cycles and cell division direction [45–48]. Our study argued that *Np63* play an important role in basal

cells for corneal epithelial innervation. The exact mechanism by which Np63 regulated corneal innervation was not clear. The results of RNAi of *Np63* reduced Ngf synthesis in TKE2 cells (Fig.8A) and the downregulation of *Np63* and *Ngf* expression in the cornea of *Shp2<sup>K14ce-cko</sup>* mice (Fig.8B) suggested that soluble factor(s) such as Ngf may be associated with the corneal denervation in vivo and impairment of neurite outgrowth in co-culture system. We also have performed preliminary RNAseq analysis and found that the expression of nerve growth factor (*NGF*), brain-derived neurotrophic factor (*BDNF*), semaphorin (*Sema*) 6B, 4D and 6D was significantly down-regulated in *Shp2* siRNA or *Np63* siRNA-treated TKE2 cells, while the expression of *Sema* 3D, 5A, 7A was increased (unpublished data). The role of these neurotrophic factors involved in nerve growth, maintenance, proliferation and survival [3,49–52] required further investigation in the future.

One of the interesting observations in this study was that Shp2 might strictly monitor the protein level of Np63 in epithelial basal cells. Under naïve situation, Shp2 up-regulated Np63 expression (Fig. 9A, 9C). This is consistent with several previous reports, in which signals from EGFR-induced Np63 expression in multiple cell lines [53]. More interestingly, in present study, we found that higher expression of Shp2 downregulated Np63 protein level probably through proteasome-mediated degradation (Fig. 9B). This result was in agreement with our *in vivo* data, in which overexpression of *Shp2<sup>E76K</sup>* [54] in corneal basal epithelial cells also led to corneal epithelial defects in *K14rtTA;tetO-Shp2<sup>E76K</sup>* adult mice administered with Dox chow (our unpublished data). Since Np63 protein stability is mainly regulated by ubiquitin-dependent proteasomal degradation pathway [55,56], it is likely that fine-tuning of Np63 protein level in corneal basal cells is critical to the epithelial cell stratification, maintenance and nerve innervation during development and homeostasis of cornea.

## Supplementary Material

Refer to Web version on PubMed Central for supplementary material.

## ACKNOWLEDGMENT

Supported in part by grants from NIH/NEI EY29071 (CYL); Ministry of Science and Technology (MOST) grant (Taiwan) 1042314B182A097MY3 (LKY); and Chang Gung Medical Research Project grants: CMRPG3E1522 (LKY); CMRPG3H1381 (LKY). We thank Hui-Chun Kung and Ya-Ling Chen for preparation of TEM studies at the Microscope Center of Chang-Gung Memorial Hospital, Linko, Taiwan.

## REFERENCES

1. Hassell JR, Birk DE. The molecular basis of corneal transparency. *Exp. Eye Res.* 2010;91:326–35. [PubMed: 20599432]
2. Müller LJ, Marfurt CF, Kruse F, Tervo TMT. Corneal nerves: structure, contents and function. *Exp. Eye Res.* 2003;76:521–42. [PubMed: 12697417]
3. Kubilus JK, Linsenmayer TF. Developmental guidance of embryonic corneal innervation: Roles of Semaphorin3A and Slit2. *Dev. Biol.* 2010;344:172–84. [PubMed: 20471970]
4. Müller LJ, Vrensen GF, Pels L, Cardozo BN, Willekens B. Architecture of human corneal nerves. *Invest. Ophthalmol. Vis. Sci.* 1997;38:985–94. [PubMed: 9112994]
5. Shaheen BS, Bakir M, Jain S. Corneal nerves in health and disease. *Surv. Ophthalmol.* 2014; 59:263–85. [PubMed: 24461367]

6. Mckenna CC, Lwigale PY. Innervation of the mouse cornea during development. *Investig. Ophthalmol. Vis. Sci.* 2011;52:30–5. [PubMed: 20811061]
7. Kubilus JK, Linsenmayer TF. Developmental corneal innervation: Interactions between nerves and specialized apical corneal epithelial cells. *Investig. Ophthalmol. Vis. Sci.* 2010;51:782–89. [PubMed: 19741242]
8. Marfurt CF, Kingsley RE, Echtenkamp SE. Sensory and sympathetic innervation of the mammalian cornea. A retrograde tracing study. *Invest. Ophthalmol. Vis. Sci.* 1989;30:461–72. [PubMed: 2494126]
9. Lwigale PY. Embryonic Origin of Avian Corneal Sensory Nerves. *Dev. Biol.* 2001; 239:323–37. [PubMed: 11784038]
10. Müller LJ, Pels L, Vrensen GF. Ultrastructural organization of human corneal nerves. *Invest. Ophthalmol. Vis. Sci.* 1996;37:476–88. [PubMed: 8595948]
11. Stepp MA, Tadvalkar G, Hakh R, Pal-Ghosh S. Corneal Epithelial Cells Function as Surrogate Schwann Cells for their Sensory Nerves. *Glia* 2017;65:851–63. [PubMed: 27878997]
12. Baker KS, Anderson SC, Romanowski EG, Thoft RA, SundarRaj N. Trigeminal ganglion neurons affect corneal epithelial phenotype. Influence on type VII collagen expression in vitro. *Invest. Ophthalmol. Vis. Sci.* 1993; 34:137–44. [PubMed: 7678833]
13. Garcia-Hirschfeld J, Lopez-Briones LG, Belmonte C. Neurotrophic Influences on Corneal Epithelial Cells. *Exp. Eye Res.* 1994;59:597–605. [PubMed: 9492761]
14. Reid TW., Murphy CJ., Iwahashi CK., Foster BA. & Mannis MJ. Stimulation of epithelial cell growth by the neuropeptide substance P. *J. Cell. Biochem.* 1993;52:476–85. [PubMed: 7693729]
15. Chan KY, Haschke RH. Isolation and culture of corneal cells and their interactions with dissociated trigeminal neurons. *Exp. Eye Res.* 1982;35:137–56. [PubMed: 7151883]
16. Chan KY, Jones RR, Bark DH, Swift J, Parker JA Jr, Haschke RH. Release of neuronotrophic factor from rabbit corneal epithelium during wound healing and nerve regeneration. *Exp. Eye Res.* 1987;45:633–46. [PubMed: 3428389]
17. Oswald DJ, Lee A, Trinidad M, Chi C, Ren R, Rich CB, et al. Communication between Corneal Epithelial Cells and Trigeminal Neurons Is Facilitated by Purinergic (P2) and Glutamatergic Receptors. *PLoS One* 2012;7:e44574. [PubMed: 22970252]
18. Canner JP, Linsenmayer TF, Kubilus JK. Developmental regulation of trigeminal TRPA1 by the cornea. *Invest. Ophthalmol. Vis. Sci.* 2014;56:29–36. [PubMed: 25503452]
19. Bonini S, Rama P, Olzi D, Lambiase A. Neurotrophic keratitis. *Eye* 2003;17:989–95. [PubMed: 14631406]
20. Davis EA, Dohlman CH. Neurotrophic keratitis. *Int. Ophthalmol. Clin.* 2001;41:1–11.
21. Mastropasqua L, Massaro-Giordano G, Nubile M, Sacchetti M. Understanding the Pathogenesis of Neurotrophic Keratitis: The Role of Corneal Nerves. *J. Cell. Physiol.* 2017;232:717–24. [PubMed: 27683068]
22. Sacchetti M, Lambiase A. Diagnosis and management of neurotrophic keratitis. *Clin. Ophthalmol.* 2014;8:571–9. [PubMed: 24672223]
23. Versura P, Giannaccare G, Pellegrini M, Sebastiani S, Campos EC. Neurotrophic keratitis: current challenges and future prospects. *Eye Brain* 2018;10:37–45. [PubMed: 29988739]
24. Ng GY, Yeh LK, Zhang Y, Liu H, Feng GS, Kao WW et al. Role of SH2-containing tyrosine phosphatase Shp2 in mouse corneal epithelial stratification. *Invest. Ophthalmol. Vis. Sci.* 2013;54:7933–42. [PubMed: 24204042]
25. Freeman RM Jr, Plutzky J, Neel BG. Identification of a human src homology 2-containing protein-tyrosine-phosphatase: a putative homolog of *Drosophila* corkscrew. *Proc. Natl. Acad. Sci. U. S. A.* 1992;89:11239–43. [PubMed: 1280823]
26. Jamieson CR, van der Burgt, Brady AF, van Reen M, Elsayi MM, Hol F et al. Mapping a gene for Noonan syndrome to the long arm of chromosome 12. *Nat. Genet.* 1994;8:357–60. [PubMed: 7894486]
27. Chan RJ, Feng GS. PTPN11 is the first identified proto-oncogene that encodes a tyrosine phosphatase. *Blood* 2007;109:862–67. [PubMed: 17053061]

28. Dance M, Montagner A, Salles JP, Yart A, Raynal P. The molecular functions of Shp2 in the Ras/Mitogen-activated protein kinase (ERK1/2) pathway. *Cell. Signal.* 2008;20:453–9. [PubMed: 17993263]
29. Matozaki T, Murata Y, Saito Y, Okazawa H, Ohnishi H. Protein tyrosine phosphatase SHP-2: A proto-oncogene product that promotes Ras activation. *Cancer Sci.* 2009;100:1786–93. [PubMed: 19622105]
30. Grossmann KS, Rosário M, Birchmeier C, Birchmeier W. The tyrosine phosphatase Shp2 in development and cancer. *Adv Cancer Res* 2010;106:53–89. [PubMed: 20399956]
31. Nguyen H, Rendl M, Fuchs E. Tcf3 Governs Stem Cell Features and Represses Cell Fate Determination in Skin. *Cell* 2006;127:171–83. [PubMed: 17018284]
32. Perl AK, Wert SE, Nagy A, Lobe CG, Whitsett JA. Early restriction of peripheral and proximal cell lineages during formation of the lung. *Proc. Natl. Acad. Sci. U. S. A.* 2002;99:10482–7. [PubMed: 12145322]
33. Feng G, Mellor RH, Bernstein M, Keller-Peck C, Nguyen QT, Wallace M, et al. Imaging neuronal subsets in transgenic mice expressing multiple spectral variants of GFP. *Neuron* 2000;28:41–51. [PubMed: 11086982]
34. Zhang EE, Chapeau E, Hagihara K, Feng GS. Neuronal Shp2 tyrosine phosphatase controls energy balance and metabolism. *Proc. Natl. Acad. Sci.* 2004;101:16064–69. [PubMed: 15520383]
35. Aykut V, Elbay A, Çigdem Uçar, Esen F, Durmus A, Karadag R et al. Corneal sensitivity and subjective complaints of ocular pain in patients with fibromyalgia. *Eye (Lond).* 2018;32:763–67. [PubMed: 29386615]
36. Okada Y, Sumioka T, Ichikawa K, Sano H, Nambu A, Kobayashi K et al. Sensory nerve supports epithelial stem cell function in healing of corneal epithelium in mice: the role of trigeminal nerve transient receptor potential vanilloid 4. *Lab. Investig.* 2019;99:210–30. [PubMed: 30413814]
37. Kubota M, Shimmura S, Miyashita H, Kawashima M, Kawakita T, Tsubota K. et al. The Anti-oxidative Role of ABCG2 in Corneal Epithelial Cells. *Investig. Ophthalmology Vis. Sci.* 2010;51:5617–22.
38. Vandewauw I, Owsianik G, Voets T. Systematic and quantitative mRNA expression analysis of TRP channel genes at the single trigeminal and dorsal root ganglion level in mouse. *BMC Neurosci.* 2013;14:21. [PubMed: 23410158]
39. Suzuki M, Mizuno A, Kodaira K, Imai M. Impaired Pressure Sensation in Mice Lacking TRPV4. *J. Biol. Chem.* 2003;278:22664–68. [PubMed: 12692122]
40. Aceto N, Sausgruber N, Brinkhaus H, Gaidatzis D, Martiny-Baron G, Mazarol G. et al. Tyrosine phosphatase SHP2 promotes breast cancer progression and maintains tumor-initiating cells via activation of key transcription factors and a positive feedback signaling loop. *Nat. Med.* 2012;18:529–37. [PubMed: 22388088]
41. Ferrari G1, Chauhan SK, Ueno H, Nallasamy N, Gandolfi S, Borges L. et al. A Novel Mouse Model for Neurotrophic Keratopathy: Trigeminal Nerve Stereotactic Electrolysis through the Brain. *Invest Ophthalmol Vis. Sci.* 2011;52:2532–9.
42. Wong EK, Kinyamu RD, Graff JM, Chak G, Wong MN, Agnic H et al. A rat model of radiofrequency ablation of trigeminal innervation via a ventral approach with stereotaxic surgery. *Exp. Eye Res.* 2004;79:297–303. [PubMed: 15336491]
43. McKenna CC, Lwigale PY. Innervation of the mouse cornea during development. *Invest. Ophthalmol. Vis. Sci.* 2011;52:30–5. [PubMed: 20811061]
44. He J, Bazan HE. Neuroanatomy and neurochemistry of mouse cornea. *Invest Ophthalmol. Vis. Sci.* 2016;57:664–74. [PubMed: 26906155]
45. Koster MI, Roop DR. Mechanisms regulating epithelial stratification. *Annu. Rev. Cell Dev. Biol.* 2007;23:93–113. [PubMed: 17489688]
46. Shalom-Feuerstein R, Lena AM, Zhou H, De La Forest Divonne S, Van Bokhoven H, Candi E, Melino G et al. Np63 is an ectodermal gatekeeper of epidermal morphogenesis. *Cell Death Differ.* 2011;18:887–96. [PubMed: 21127502]
47. Zhang Y, Yeh LK, Zhang S, Call M, Yuan Y, Yasunaga M et al. Wnt/ $\beta$ -catenin signaling modulates corneal epithelium stratification via inhibition of Bmp4 during mouse development. *Development* 2015;142:3383–93. [PubMed: 26443636]

48. Zhang Y, Call MK, Yeh LK, Liu H, Kochel T, Wang IJ et al. Aberrant expression of a  $\beta$ -catenin gain-of-function mutant induces hyperplastic transformation in the mouse cornea. *J. Cell Sci.* 2010;123:1285–94. [PubMed: 20332116]
49. Barbieri CE, Tang LJ, Brown KA, Pietenpol JA. Loss of p63 Leads to Increased Cell Migration and Up-regulation of Genes Involved in Invasion and Metastasis. *Cancer Res.* 2006;66:7589–97. [PubMed: 16885358]
50. Kobayashi T, Shiraishi A, Hara Y, Kadota Y, Yang L, Inoue T. et al. Stromal-epithelial interaction study: The effect of corneal epithelial cells on growth factor expression in stromal cells using organotypic culture model. *Exp. Eye Res.* 2015;135:109–17. [PubMed: 25682729]
51. Uren RT, Turnley AM. Regulation of neurotrophin receptor (Trk) signaling: suppressor of cytokine signaling 2 (SOCS2) is a new player. *Front. Mol. Neurosci.* 2014;7:39. [PubMed: 24860421]
52. Koncina E, Roth L, Gonthier B, Bagnard D. in *Axon Growth and Guidance* 621, 50–64 (Springer New York, 2007).
53. Chu WK, Lee KC, Chow SE, Chen JK. Dual regulation of the Np63 transcriptional activity by Np63 in human nasopharyngeal carcinoma cell. *Biochem. Biophys. Res. Commun.* 2006;342:1356–60. [PubMed: 16516862]
54. Schneeberger VE, Luetke N, Ren Y, Berns H, Chen L, Foroutan P, et al. SHP2E76K mutant promotes lung tumorigenesis in transgenic mice. *Carcinogenesis.* 2014;35:1717–25. [PubMed: 24480804]
55. Li C, Xiao ZX. Regulation of p63 protein stability via ubiquitin-proteasome pathway. *Biomed Res. Int.* 2014;2014:175721. [PubMed: 24822180]
56. Armstrong SR, Wu H, Wang B, Abuetabh Y, Sergi C, Leng RP. The Regulation of Tumor Suppressor p63 by the Ubiquitin-Proteasome System. *Int. J. Mol. Sci.* 2016;17:pii:E2041. [PubMed: 27929429]

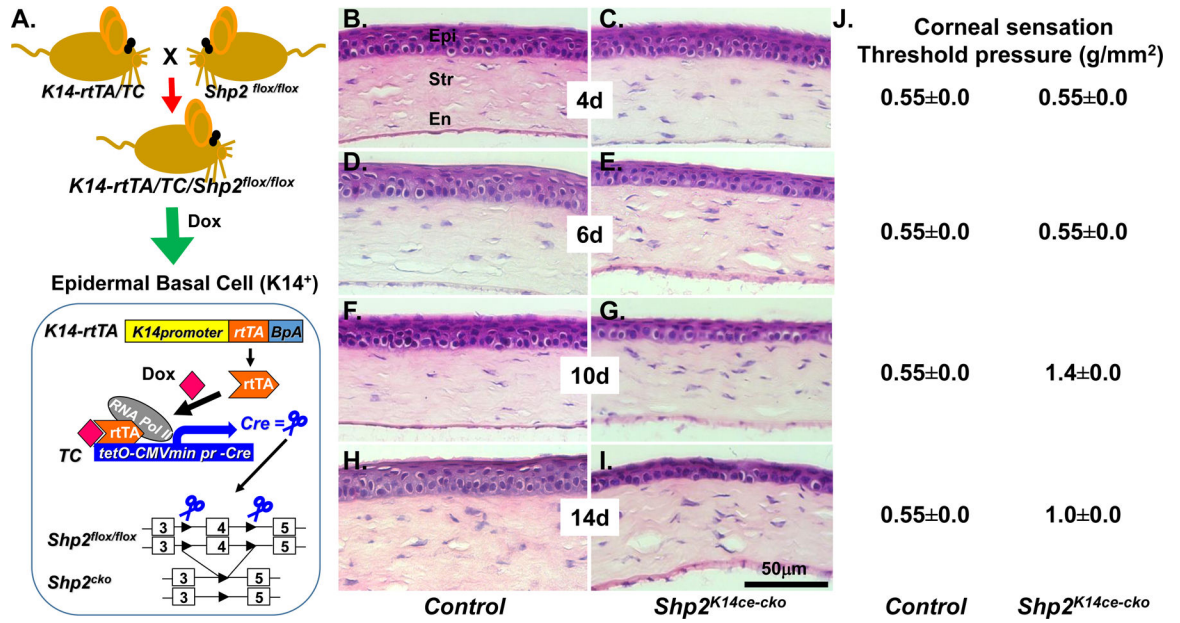


**Fig. 1. *Shp2* is essential for corneal epithelial homeostasis.**

(A) Schematic representation of Dox-inducible ablation of *Shp2* gene specifically in K14 expressing cells including the corneal basal cells of the triple transgenic mice (*K14-rtTA*/*TC*/*Shp2*<sup>flx/flx</sup>). (B-I) H&E staining showed that the corneal epithelial thickness of the triple transgenic mice (C, E, G, I) was gradually reduced after Dox induction for 4, 6, 10 and 14 days, respectively since P60 compared with litter controls (B, D, F, H). Note that the central corneal epithelial cell layers did not change dramatically after 4 days of Dox induction (C). Cell layers significantly deduced since 6 days Dox induction (E). In contrast, control mice kept 6–7 stratified corneal epithelial cell layers after Dox induction. (J), Functional assay of corneal sensation were measured in three mice (6 eyes) of each time point by Cochet-Bonnet aesthesiometer. Corneal sensitivity significantly reduced from 0.55±0.0 to 1.4±0.0 and 1.0±0.0 (g/mm<sup>2</sup>) at 10 and 14 days, respectively, after Dox administration. (N=6, *P*<0.01). Abbreviations: Epi: corneal epithelium; Str, stroma; En, endothelium.

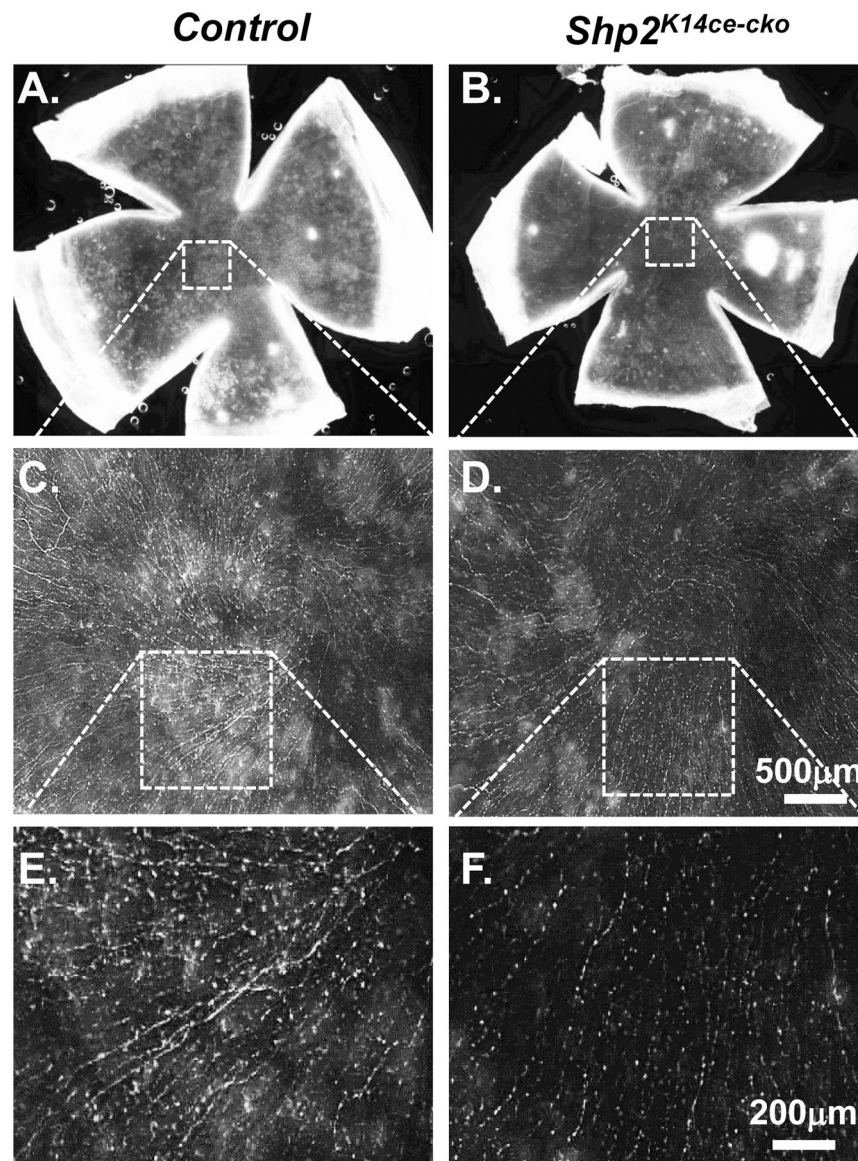


**Fig. 2. *Shp2* deletion in corneal basal epithelial cells reduced nerve innervation density in corneal epithelium.**

(A, B) Representative whole mount overviews of mouse corneal epithelial nerve innervation from adult mice administered Dox for 10 days. (C-F) Detail structure of central corneal nerve networks. Note that *Shp2* deficiency resulted in lower density of corneal epithelial nerve fibers/bundles (compare D to C; F to E). In addition, Three mice (N= 6 corneas) of each group were examined. *Shp2* deficiency caused less nerve fibers in corneal epithelial nerve networks (compare F to E).



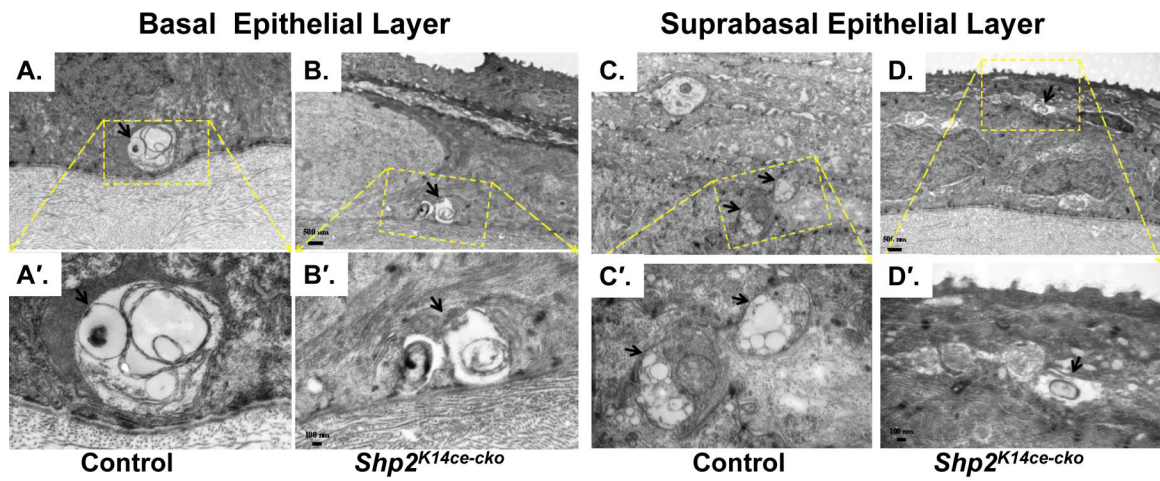


**Fig. 3. Ablation of Shp2 in CE impaired corneal nerve bundle/fiber formation.**

Transmission electron micrographs of control group (A, A', C, C') and *Shp2<sup>K14cecko</sup>* (B, B', D, D'). Control corneal epithelium exhibited healthy nerve bundles (arrow) in the epithelial basal layer (A, A') and nerve fibers (arrows) in subbasal layers (C, C'). In contrast, *Shp2<sup>K14cecko</sup>* displayed degeneration in both nerve bundles and fibers (B, B', D, D').

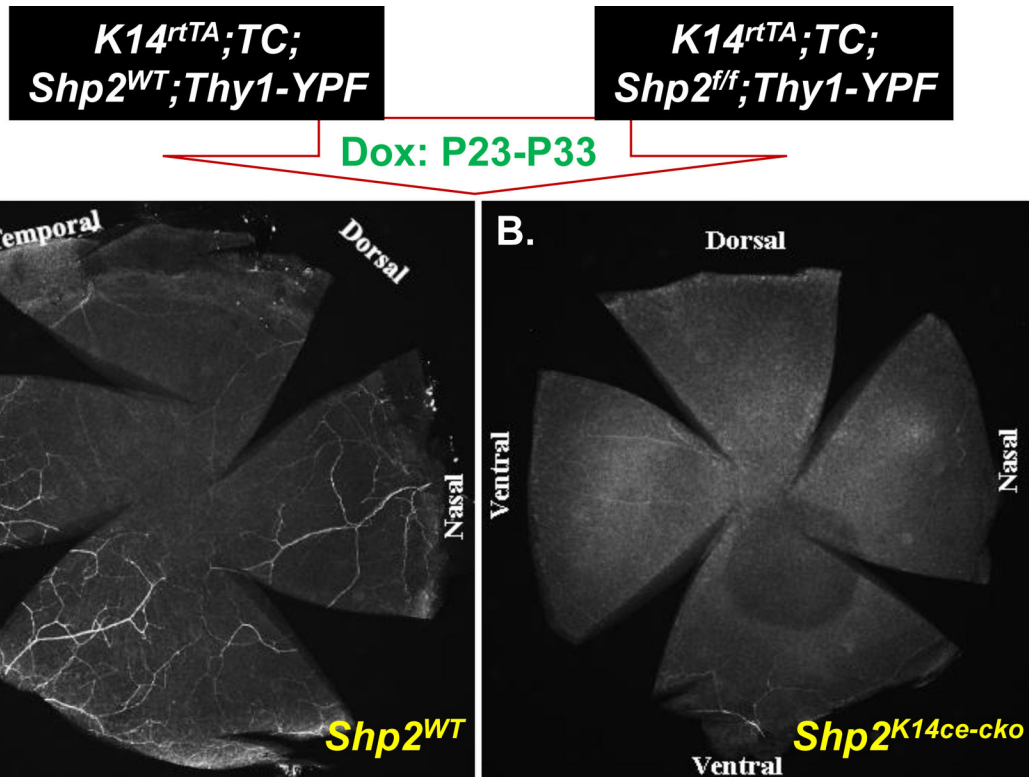


**Fig. 4. Shp2 ablation resulted in corneal denervation.** Whole-mount cornea YFP fluorescent images showed that nerve fibers were detected in *Shp2<sup>WT</sup>* (A), while YFP was fragmented or absent in *Shp2<sup>K14ce-cko</sup>* (B).

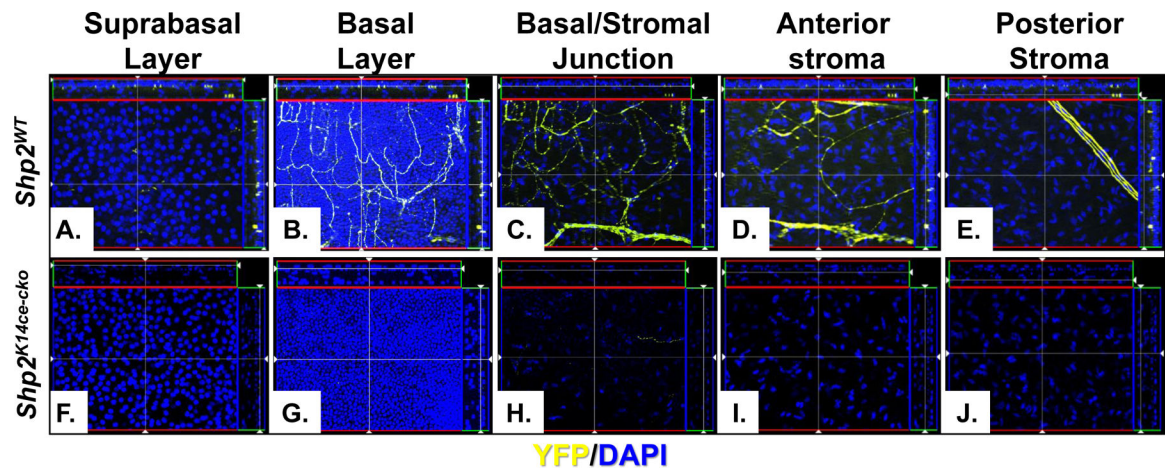


**Fig. 5. Shp2 ablation caused corneal denervation.**

Images of YFP-positive optical sections were taken by ZEISS Apotome 2 from the central cornea of *Shp2*<sup>WT</sup> (A.-E.) and *Shp2*<sup>K14ce-cko</sup> (F.-J.) mice. Note that nerve fiber branches and endings were present in the suprabasal layer, basal layer, epithelial/stromal junction, anterior and posterior stroma layer. In contrast, YFP signal was only fragmented or absent in *Shp2*<sup>K14ce-cko</sup>.

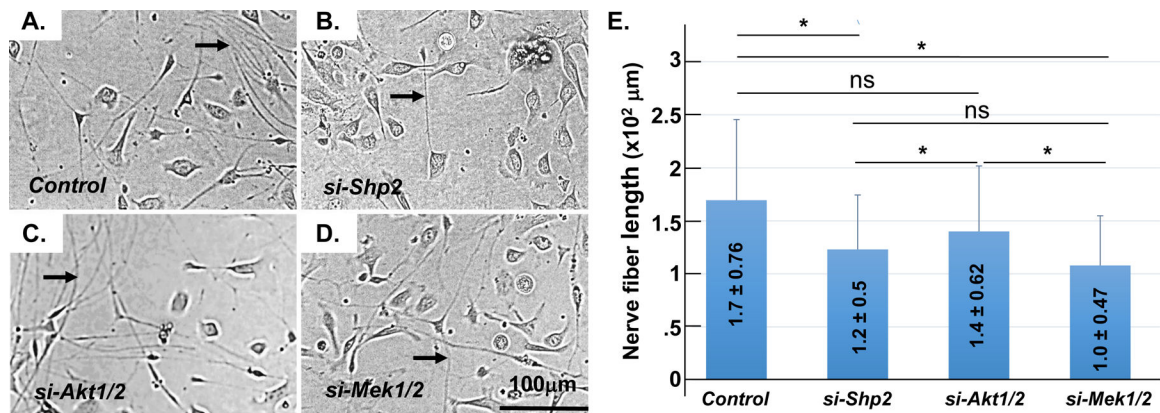


**Fig. 6. Measurement of neurite outgrowth of mouse primary TGC co-cultured with siRNA-transfected TKE2 cells.**

Micrographs showed that TKE2 transfected with *Shp2* siRNA (B) or *Mek1/2* siRNA (D) impeded TGC neurite outgrowth as compared with control siRNA-transfected TKE2 (A). However, TKE2 transfected with *Akt1/2* siRNA (C) had no significant change on the neurite outgrowth (compare C with A). Arrows indicate neurite fibers (A-D). Histogram presentation of images of A-D (E). Three independent experiments have been performed. \*: (N=90,  $P < 0.05$ ); NS: no significance.

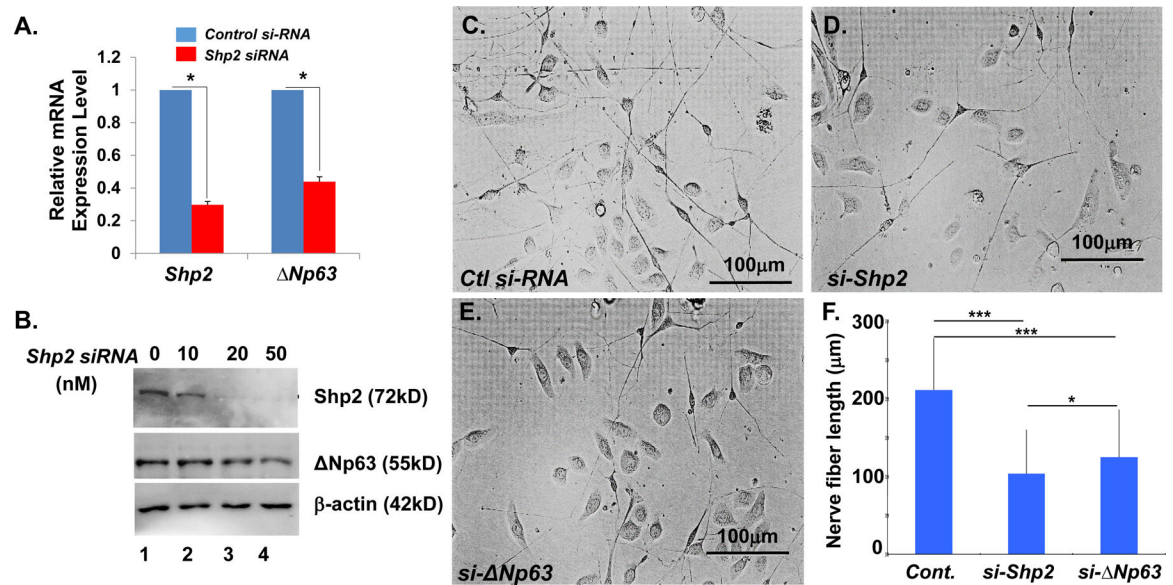


**Fig. 7. Either *Shp2* or *Np63* knockdown in TKE2 cells by siRNA transfection impeded neurite outgrowth of co-cultured primary TGCs.**

(A) RT-qPCR analysis of *Shp2* and *Np63* mRNA in TKE2 cells treated with control (*Ctl*) or *Shp2* siRNA (10nM) for 48hrs. \*: N=4,  $p < 0.05$ . (B) Western blotting analysis of Shp2,

*Np63*, and  $\beta$ -actin in TKE2 cells transfected with 0, 10, 20, and 50nM of *Shp2* siRNA for 48hrs, respectively. (C-E) Micrographs showed that TKE2 transfected with *Shp2* siRNA (*si-Shp2*, D) or *Np63* siRNA (*si- $\Delta Np63$* , E) impeded neurite outgrowth as compared with control siRNA-transfected TKE2. (F) Histogram showed TGCs nerve fiber length from three independent experiments. All data are shown as mean  $\pm$  SD. \*: (N=90,  $P < 0.05$ ) \*\*\*: (N=90,  $p < 0.005$ )

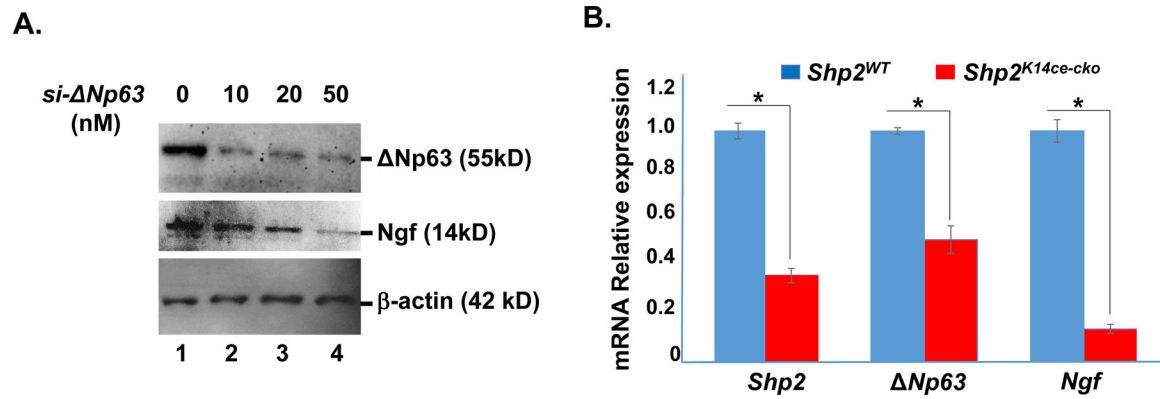


**Fig.8. Down regulation of Ngf in *Np63* siRNA-transfected TKE2 cells and in *Shp2*<sup>K14ce-cko</sup> cornea.**

(A) Western blotting analysis showed that Ngf protein expression level was decreased in *si-Np63* transfected TKE2 cells. (B) qRT-PCR analysis of *Shp2*, *Np63* and *Ngf* mRNAs in *Shp2*<sup>WT</sup> and *Shp2*<sup>K14ce-cko</sup> corneas. Note that the 35% of *Shp2* expression in the *Shp2*<sup>K14ce-cko</sup> was likely attributed to the contamination of non-epithelial tissue; nevertheless, both *Np63* and *Ngf* mRNAs were reduced dramatically in *Shp2*<sup>K14ce-cko</sup> as compared to those in *Shp2*<sup>WT</sup> controls. \*:  $P < 0.05$  (N=4)

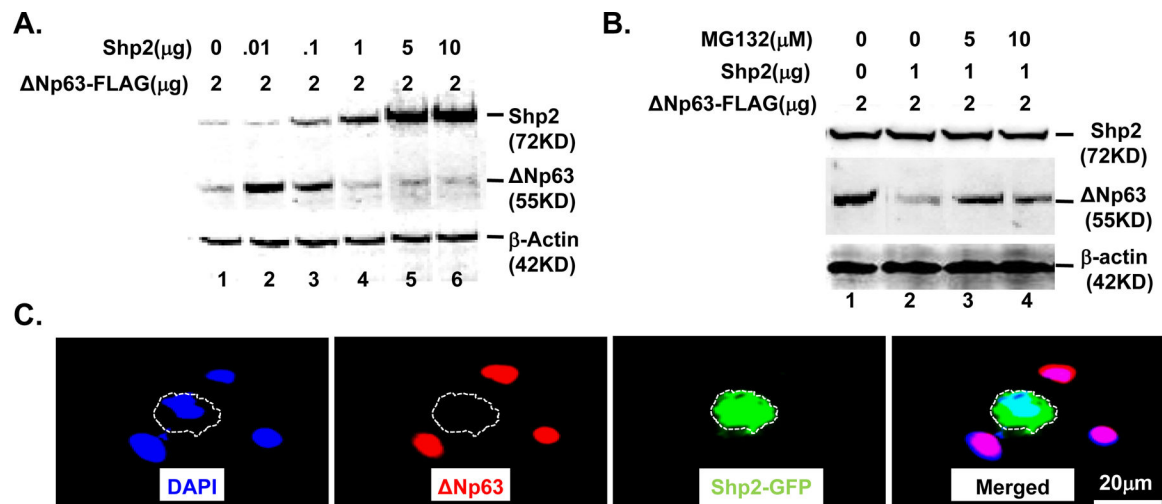


**Fig. 9. Shp2 tightly regulated Np63 protein level in HEK293 and HTCE cells.**

(A) Western blot analysis showed that Shp2 controls Np63 protein level in a dosage dependent manner in HEK293 cells. Transfection of low dosages of *Shp2* plasmid DNA (0.01–0.1 $\mu$ g) increased Np63 protein level. However, higher dosage of *Shp2* (1 $\mu$ g) decreased Np63 protein level (B). MG132, a proteasome inhibitor, attenuated the inhibitory effect of high dosage of *Shp2* to Np63 protein level. (C) Immunofluorescent staining showed that Shp2 (red) and Np63 (green) were exclusively expressed in HTCE co-transfected with *CMV-Shp2-EGFP* and *CMV-Np63* plasmid. All experiments were repeated three times and showed very similar results.

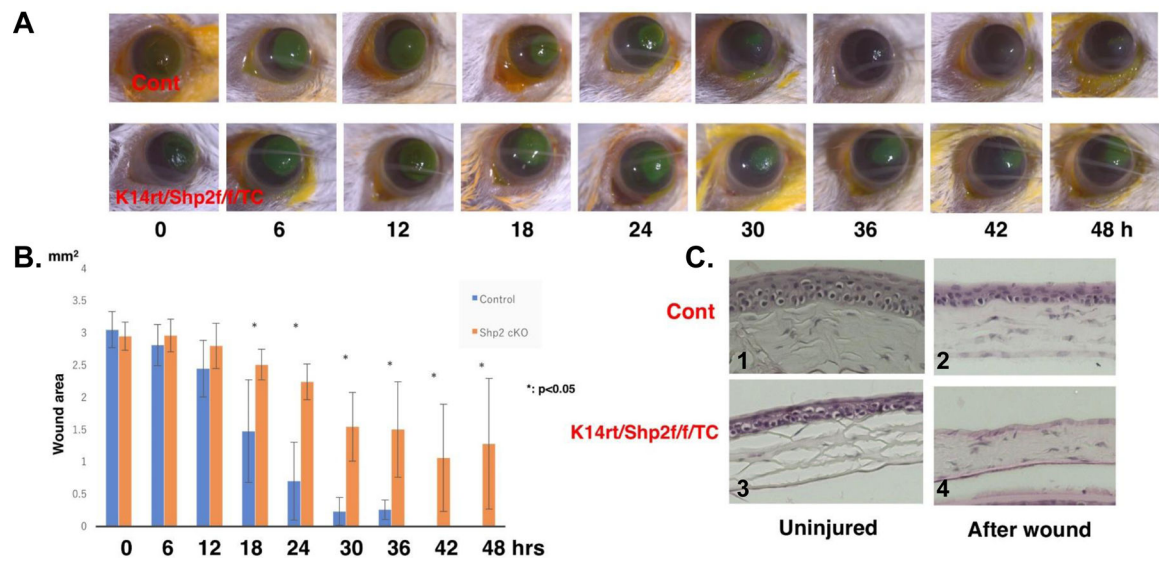


**Fig. 10. Wound healing delayed in *Shp2*<sup>K14ce-cko</sup> mice.**

(A) Photographs of corneal debridement healing process taken at different time points from 0 to 48hrs post wound. *Shp2* deficiency in corneal basal epithelial cells (lower panel of A) impaired corneal wound healing process as compared with control mice (upper panel of A). (B) Bar chart of the size of remaining epithelial defects in the corneal epithelium at each time point. (C) H&E staining showed that there were no corneal epithelial cell layer covered in the *Shp2*<sup>K14ce-cko</sup> mice (C4), while 4–5 epithelial cell layers formed in the control mice (C2) at 48hrs post wound. \*: (N=6,  $P < 0.05$ ); NS: no significance.